

EM based algorithm to infer both phenotypic state and cell division properties from lineage information

So Nakashima¹, Yuki Sughiyama², and Tetsuya J. Kobayashi^{2,3}

Abstract—Individual cells in a population generally has different reproductive ability, presumably due to the phenotypic variability of the cells. Identifying such variability in the state of the cells is crucial because the speed of the proliferation is correlated with different kinds of cellular physiology such as the resistance to stresses. Even with technological development to monitor the proliferation of single cells over hundred generations and to trace the lineage of cells, estimating the state of cells is still hampered by the lack of statistical methods that can appropriately account for the lineage specific problems. In this work, we develop a new statistical method to infer the growth-related hidden state of cells from cellular lineages, with which the information of all the cells can be used for inference with an appropriate correction of growth bias. A performance test with a synthetic data demonstrates the validity of our method. An application of our method to a lineage data of *E.coli* has identified a three dimensional effective state in the cells, one component of which seems to capture slow fluctuation of cellular state over tens of generations.

I. INTRODUCTION

The cells in a population show heterogeneous phenotypes even though they are genetically identical and a cell inherits a part of the heterogeneity from its parent cell. Such phenotypic variety is important to understand some biological phenomena. One of such phenomena is persistency, a fractional killing of bacterial populations by antibiotics [1]. While the persisters were considered as dormant cells, researchers have revealed the importance of the phenotypic variety [2], [3]. The understanding of persistency has a huge impact on the biomedicine: several researchers pointed out the similarity between the persistency of microbes and the drug-resistance of cancers [4], [5]. Another example is development. In the process of development, cells reach their own differentiated state even though they are genetically identical. Understanding the mechanism of development is a fundamental question in developmental biology and important to the biomedical application of ES and iPS cells.

Researchers have aimed to understand the effects and dynamics of such heterogeneity. One promising method is single-cell RNA sequence (scRNAseq). Single-cell RNA sequence is used to observe the heterogeneity of cells and find the phenotypic states of them [6], [7]. However, such data are snapshots of the RNA expression of the cells and lack

information about time. Another difficulty of the scRNAseq is the high-dimensionality of its data. On the other hand, lineage data of cells and organisms are becoming more and more accessible owing to the development of single-cell tracking techniques [8], [9] (Figure I.1 (a)). A lineage of cells is composed of two kinds of information: parent-daughter relationship of the cells and the times when each cell divided. Single-cell tracking is a kind-of compensatory method of scRNAseq since it provides us accurate information about time and cell division. Therefore, our goal in this paper is to reconstruct the effective heterogeneity, which we call a state, and to estimate the dynamics of the states from the lineage data (Figure I.1 (b)). This enables us to study the dynamics of the heterogeneity. Furthermore, this contributes to the analysis of scRNAseq data: we can combine abundant data of heterogeneity by scRNAseq and reconstructed dynamics of states from lineage data to analyze the more accurate dynamics of heterogeneity; in addition, we can project the high-dimensional scRNAseq data into low-dimensional states.

Reconstruction of the states from lineage data is accompanied by two difficulties. First, the states are unobservable and we have to find them from data. That is, our goal essentially contains latent variable estimation on tree-structured time-series data. This problem is intensively studied by using kin-correlation [10], [11], clustering algorithms [12], and Monte-Carlo algorithms [13]. Estimation in a tree-structured data was originally studied for image processing [14], [15]. The number of the dimension of the state is also unknown and we have to determine it from data. Model selection method like Akaike's Information Criteria (AIC) is applicable [16]. Therefore, this problem seems to be solved by a combination of existing estimation techniques at first sight. However, this naïve anticipation is wrong due to the second difficulty: usual estimation methods, like maximal likelihood estimation (MLE), suffer from growth bias and yields wrong conclusions. It is known that the average of growth-related quantities over population deviates from intrinsic cell property due to the intrapopulation competition. This deviation has been theoretically analyzed and experimentally observed [17], [9], [18] when there are no states. This problem happens in scRNAseq too. The second problem is unique to growing systems and crucial to the estimated result of latent variables. Thus, we have to establish a nice correction method. The growth bias is studied in the field of branching process [19]. Recently, the growth bias in a growing system with states began to be analyzed [20], [21]. However, this topic is still ongoing and there is no established correction method.

To overcome these difficulties, we first analyze the growth

¹ Graduate School of Information and Science, Department of Mathematical information, University of Tokyo, 7-3-1, Hongo, Bunkyo-ku, 113-8654, Japan `so_nakashima` at `mist.i.u-tokyo.ac.jp`

²Institute of Industrial Science, The University of Tokyo, 4-6-1 Komaba, Meguro-ku 153-8505, Tokyo, Japan `tetsuya` at `mail.crmind.net`

³ PRESTO, Japan Science and Technology Agency (JST), 4-1-8 Honcho Kawaguchi, Saitama 332-0012, Japan

bias in the growing system with states based on a branching process and a retrospective process. Based on this analysis, we establish a correction method of the growth bias. Then, we next propose a latent variable estimation algorithm on lineage based on an EM algorithm, which we call lineage EM algorithm (LEM). EM algorithm is a well-established latent variable estimation algorithm. We verify the effectiveness of LEM by the estimation of synthetic data. We also apply LEM to a lineage data of *E. coli*. The result of LEM suggests the existence of a slow dynamics which affects the inter-division time of *E. coli*.

II. MODELING SINGLE-CELL DYNAMICS OF DIVISION AND STATE-SWITCHING

In this paper, we use a variant of the branching process as a model of a growing population with the state switching. We consider the symmetric division upon which the mother cell turns into two daughters without death. Each cell has its state $x \in \Omega$ where Ω is either discrete or continuous. Each daughter cell switches its state stochastically upon division of the mother cell. The state switching of a daughter cell is dependent on the state of the mother but independent of the state of the other daughter. The probability to change the state from x to x' is given by a transition matrix $\mathbb{T}_F(x' | x)$, where $\sum_{x'} \mathbb{T}_F(x' | x) = 1$ (Figure III.1 (c)). For notational simplicity, we use $\sum_{x' \in \Omega}$ instead of $\int_{x' \in \Omega} dx'$ even for Ω being a continuous state space in this section. The inter-division interval τ between consecutive division is dependent on the state x of the cell, the probability distribution of which is denoted by $\pi_F(\tau | x)$ (Figure III.1 (c)).

Under this setup, by tracking all the daughter cells generated, we can obtain a lineage tree of the cell rooted by a founder cell. If we ignore one of the daughter cells randomly, we can effectively obtain a path of stochastic division and state-switching, which describes the single-cell dynamics.

III. MAIN RESULT 1: GROWTH BIAS AND ITS CORRECTION

In order to demonstrate the problem of the growth bias, we start with the situation that the state is known or experimentally observed. Under this situation, the naïve estimators of π_F and \mathbb{T}_F from data are the following empirical distributions:

$$\pi_{\text{emp}}^{\mathcal{C}}(\tau | x) := \frac{1}{|\mathcal{C}_x|} \sum_{i \in \mathcal{C}_x} \delta(\tau - \tau_i), \quad (\text{III.1})$$

$$\mathbb{T}_{\text{emp}}^{\mathcal{C}}(x' | x) := \frac{\text{number of the transitions from } x \text{ to } x'}{\text{number of the transitions from } x}, \quad (\text{III.2})$$

where the symbol $|A|$ denotes the cardinality of a finite set A , and τ_i is a generation time of cell i . \mathcal{C} is the set of all cells used for the estimation, and $\mathcal{C}_x \subset \mathcal{C}$ is the subset of the cells with state x . π_{emp} and \mathbb{T}_{emp} may converge for sufficient large number of cells in \mathcal{C} . However, the converged distributions are dependent on the way with which the cells in \mathcal{C} is sampled.

A. Chronological tracking and Forward process

The mother machine is a common system to observe the divisions of a single cell with its state switching over a long period (Figure III.1 (a)) [8]. In this system, we typically observe only the cell at the bottom of a chamber and ignore the others in it. The division and state-switching dynamics obtained in this way is described by the single-cell dynamics we already introduced in II. We can see that π_{emp} converges to π_F and \mathbb{T}_{emp} to \mathbb{T}_F . In the case that the full information of all cells in a lineage is available, the same data set can be obtained by tracking a cell in a time-forward manner, in which one of the daughter cells are randomly chosen when their mother divides (Figure III.1 (a)). In order to distinguish π_F and \mathbb{T}_F from the other converged distributions, we specifically call the dynamics generated by π_F and \mathbb{T}_F , a forward process. The convergence property of the forward process is exactly what we expect.

However, the chronological sampling has some disadvantages in terms of the estimation. First, the observation should be terminated by the death of the tracked cell. Second, the tracked cell especially with the mother machine may be exposed to a distributed environment, because the bottom of the chamber is far from the flowing medium. Finally, the chronological tracking may requires a long time for sampling a rare state into which the cell switches very rarely. If such state induces much faster replication, cells with that state may have a bigger impact than that expected from the chronological tracking.

B. Retrospective sampling and retrospective process

Another way to observe a growing population is the dynamic flow cytometer (Figure III.1 (b)) [9]. With this system, we can observe multiple cells in a population in a more spacious chamber. In the previous works by Wakamoto, a cell was retrospectively tracked from the end of the experiment, which gave a retrospective path of the cell divisions. They demonstrated that the inter-division distribution is biased by this retrospective sampling. It should be noted that states of the cell and its influence to the inter-division interval were not considered in these works. We extended their work to include state-switching by proving that the empirical distributions of the inter-division interval and the state-transition converge to $\pi_B(\tau | x)$ and $\mathbb{T}_B(x' | x)$, which constitutes a retrospective process. $\pi_B(\tau | x)$ and $\mathbb{T}_B(x' | x)$ are biased from the forward process, $\pi_F(\tau | x)$ and $\mathbb{T}_F(x' | x)$. We have proved that $\pi_B(\tau | x)$ is exponentially biased from $\mathbb{T}_F(x' | x)$ as

$$\pi_B(\tau | x) = \frac{\pi_F(\tau | x)e^{-\lambda\tau}}{Z(x)}, \quad (\text{III.3})$$

where λ is the population growth rate of the cells, and $Z(x)$ is a normalization factor. This is a direct extension of the Wakamoto's result without considering phenotypic state.

We also have proven that the state-transition matrix of the retrospective process, $\mathbb{T}_B(x' | x)$, is biased as

$$\mathbb{T}_B(x' | x) = \frac{u(x')\mathbb{T}_F(x' | x)Z(x)}{u(x)}, \quad (\text{III.4})$$

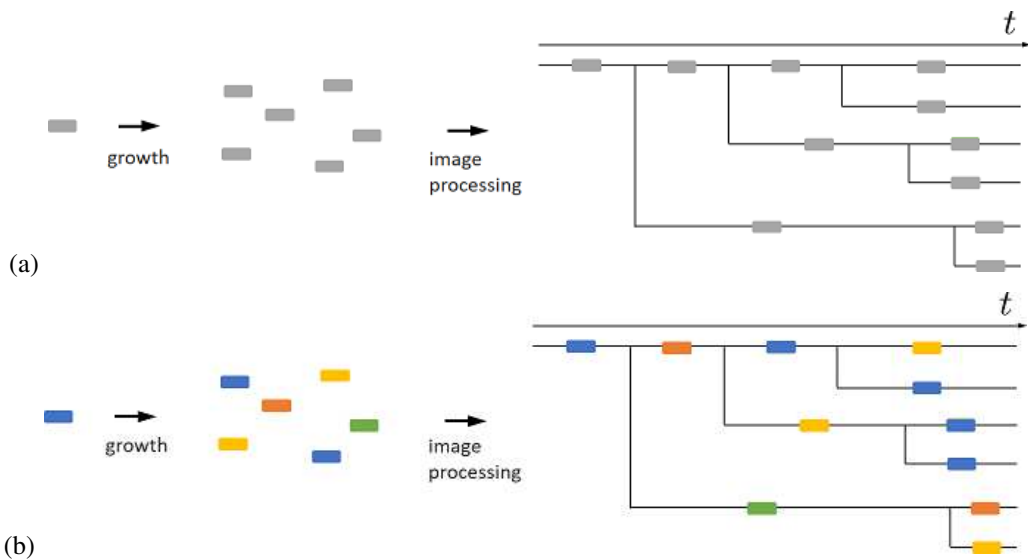


Fig. I.1: (a) A lineage of cells is composed of two kinds of information: parent-daughter relationship of the cells and the times when each cell divided. A lineage data is obtained by an image processing of the microscopic images of the growing cells. (b) Even if the cells are genetically identical, they may show heterogeneity. Such heterogeneity is considered as a bet-hedging strategy and important to understand phenomena like persistence.

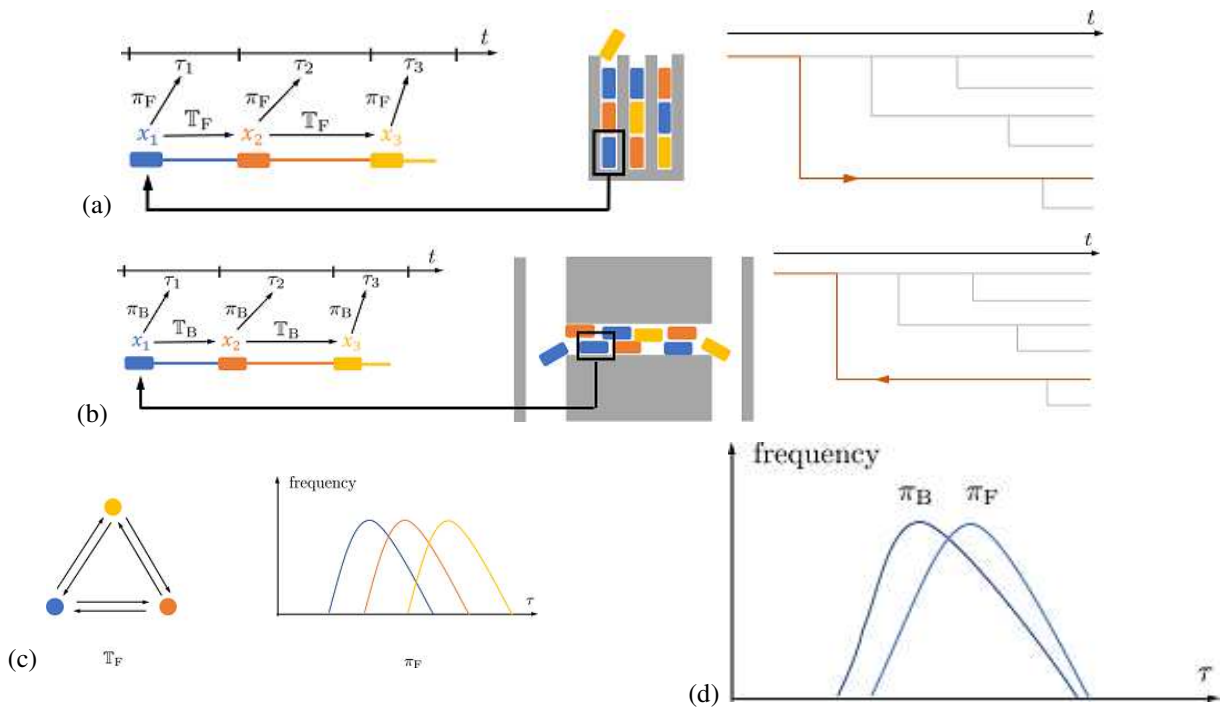


Fig. III.1: (a) A forward process. This process is obtained as a random forward path in a lineage. In a forward process, the state of a daughter is inherited from its parent. This inheritance is characterized by \mathbb{T}_F . A generation time of a cell follows a type-dependent distribution π_F . A forward process is observed by a mother machine. (b) A retrospective process. This process is obtained as an ancestral path from a cell at the end of a lineage. A retrospective process is characterized by π_B and \mathbb{T}_B . A retrospective process is observed via a dynamic cytometer. (c) Transition matrix \mathbb{T}_F governs the law of state transition. The distribution π_F determines the relative frequency of a generation time of a cell. The colors represent the states. (d) The distribution of generation time of a forward process and a retrospective process. A cell divides faster in a retrospective process than in a forward process.

TABLE III.1: Comparison of a forward process, a naive estimator of lineage data, and a retrospective process.

| | forward | retrospective | lineage |
|------------------|----------------|----------------|----------------|
| generation time | π_F | π_B | π_B |
| state transition | \mathbb{T}_F | \mathbb{T}_B | \mathbb{T}_F |

where u is the largest left eigenvector of the matrix

$$M(x' | x) := Z(x)\mathbb{T}_F(x' | x). \quad (\text{III.5})$$

Since the eigenvalue of u is unit, \mathbb{T}_B is normalized and works as a stochastic transition matrix. See Supplementary Information for the details on retrospective processes.

Because the tracked cell is selected from a population of the cells after growth, the retrospective sampling provides us with more chance to sample a rare but fast replicating states, because such states are overrepresented in the population at the end of an experiment. When only the inter-division interval is considered, the single-cell dynamics is inferred by converting π_B to π_F via (III.3). This conversion can be seen as a correction of the growth bias in the retrospective sampling. When state-switching is additionally considered, however, the retrospective sampling is accompanied by a severe drawback that we have to estimate $u(x)$ to reconstruct $\mathbb{T}_F(x' | x)$ from the estimated $\mathbb{T}_B(x' | x)$.

C. Estimation by exploiting all the cells in a lineage

In addition to the drawback, another problem shared by the chronological and retrospective samplings is that only a path of the tracked cell is used for the estimation, which requires us to conduct quite a long-term tracking to gain a sufficiently large number of sample points, i.e., cell division and state-switching events. In the case of the dynamic flow cytometer, especially, it seems a huge waste of data to abandon the information of the non-tracked cells.

We resolved this problem by proposing the lineage sampling for estimation, in which all the cells but the leaves in the lineage are used instead of those in a chronological or retrospective path. Here, the leaves correspond to the cells, the inter-division intervals of which are not observed, e.g., by the termination of the experiment or flown out from the chamber. For constructing such method, we have to clarify the converged distributions of the empirical distributions, π_{emp} and \mathbb{T}_{emp} . By using many-to-one formulae [18], [20], we have proven that π_{emp} converges to π_B , whereas \mathbb{T}_{emp} does to \mathbb{T}_F . See Supplementary information for the proof.

Owing to the direct convergence of \mathbb{T}_{emp} to \mathbb{T}_F in the lineage sampling, we can circumvent the difficulty of reconstructing \mathbb{T}_F from π_B , while enjoying the large number of sample points in the lineage. It should be noted that the problem of the limited amount of sample points cannot be avoided by tracking multiple short chronological or retrospective paths; because we have to select the cell to track from the stationary distribution of the forward or retrospective process. These stationary distributions are different from the snapshot distributions of the population. The converged distributions of chronological, retrospective, and lineage samples are summarized in Table III.1.

IV. MAIN RESULT 2: ESTIMATION FROM LINEAGE DATA WITH UNKNOWN STATES

In the preceding section, we have clarified the convergence distributions for different sampling under the situation that the states of the cells as well as inter-division intervals are available. However, the information of the states of the cells may not always be accessible. In addition, even though the states of the cells are observable experimentally, the naive estimates may require a huge amount of the sample points if the observed state space such as a collection of expressed genes or Laman spectrum is high-dimensional. Moreover, if a combination of multiple genes influences the division and state transition of the cells, we have to further search for such combination.

We resolve this problem by regarding the state of the cell, x , as a hidden state. By extending EM algorithms [22] for hidden Markov models, we construct an algorithm, Lineage EM algorithm (LEM), for estimating the lineage with a hidden state. To this end, we introduce the following parametric models with discrete or continuous state spaces, which enables us to employ well-established methods, e.g. MLE, for the estimation.

A. A parametric discrete state space model

For a discrete state space model, we assume that π_F belongs to an exponential family. The exponential families include a broad range of probability distributions such as gamma-distributions and log-normal distributions, which are prevailing distributions for fitting the inter-division intervals of microbes. By assuming a parametric model, the estimation of $\pi_F(\tau | x)$ is reduced to the set of parameters of the model. In this paper, we assume that the inter-division interval follows a gamma distribution,

$$\mathbb{P}_G(\tau; \boldsymbol{\theta}) = \frac{b^a}{\Gamma(a)} \tau^{a-1} e^{-b\tau}, \quad (\text{IV.1})$$

where $\Gamma(a)$ is the gamma function and $\boldsymbol{\theta} := (a, b)$ in which a and b are the shape and scaling parameters. Then, the state dependency of the inter-division interval for the forward process is represented by a set of parameters $\boldsymbol{\theta}_x^F = (a_x, b_x)$, and $\pi_F(\tau | x)$ is described as

$$\pi_F(\tau | x) = \mathbb{P}_G(\tau; \boldsymbol{\theta}_x^F) \quad (\text{IV.2})$$

When $\pi_F(\tau | x)$ is a gamma distribution, so is π_B with a different parameter $\boldsymbol{\theta}_x^B$ as

$$\pi_B(\tau | x) = \mathbb{P}_G(\tau; \boldsymbol{\theta}_x^B) \quad (\text{IV.3})$$

Thereby, we can convert $\boldsymbol{\theta}_x^B$ to $\boldsymbol{\theta}_x^F$ via (III.1) after estimating π_B . Hence, the estimation is reduced to the estimation of the parameters $\boldsymbol{\theta}_x^B$.

B. A parametric continuous state space model

Suppose that the continuous state space Ω is k -dimensional as $\Omega \subseteq \mathbb{R}^k$. Because the estimation considering all the possible continuous state dynamics is practically infeasible,

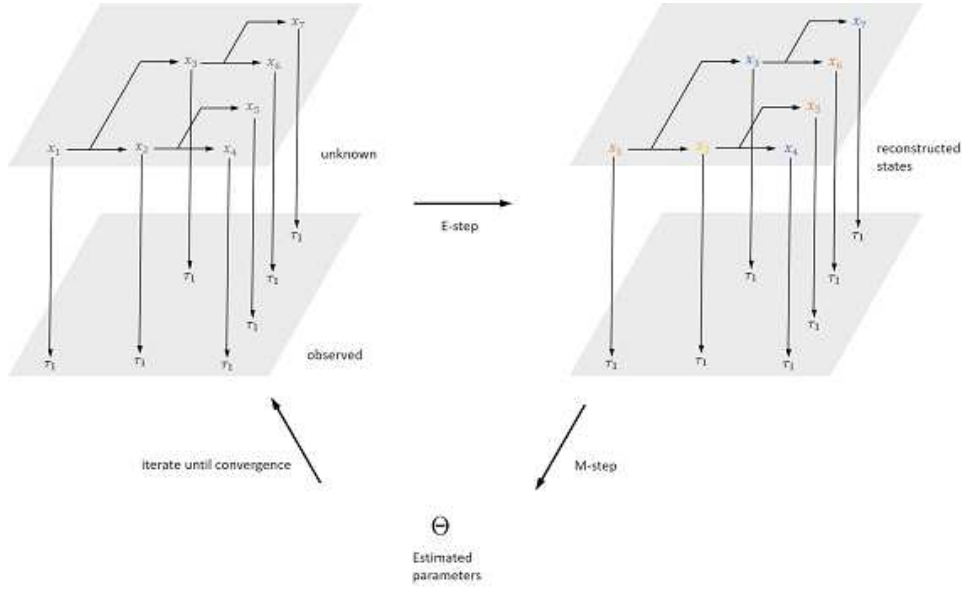


Fig. IV.1: Estimation by BW algorithm on a lineage. The dependence of states and generation time of the cells are shown as a graphical model. The state of the cells are unknown. In E-step, the unknown states are reconstructed and we obtain the posterior probability of the states. Then, in M-step, we update the parameters from the reconstructed states. This process is iterated until convergence.

we consider a linear dynamics for the state-transition, \mathbb{T}_F , which is characterized by $k \times k$ matrix \mathbf{A} as

$$\mathbf{x}' = \mathbf{A}\mathbf{x} + \mathbf{w}, \quad (\text{IV.4})$$

where \mathbf{x} and \mathbf{x}' are the states of a mother and its daughter cells, respectively. \mathbf{w} is a multidimensional Gaussian random variable with a mean vector $\mathbf{0}$ and a covariance matrix Σ_w . The retrospective distribution of the inter-division interval τ of a cell in a state \mathbf{x} , π_B , is also assumed to follow a log-normal distribution:

$$\log \tau = \mathbf{C}\mathbf{x} + v, \quad (\text{IV.5})$$

where \mathbf{C} is a $1 \times k$ matrix and v is a Gaussian random variable with mean of 0 and variance Σ_v . In this model, the estimation is to estimate parameters \mathbf{A} , \mathbf{C} , Σ_w , and Σ_v . This setting can be seen as a linear approximation of a general continuous state model.

C. Lineage EM algorithm

To obtain LEM, we extend the Baum-Welch algorithm (BW algorithm) to estimate θ_x^B and \mathbb{T}_F from lineage data (Figure IV.1). The LEM algorithm iterates two steps, E-step and M-step, and updates the parameters until convergence. Let $\Theta^{(k)}$ denote the parameters $(\mathbb{T}_F, \{\theta_x^B\})$ after the k -th iteration. In E-step, we compute the posterior probabilities for all the pairs of mother and daughter cells, $\xi_{i,j}(x, x')$, conditioned on the currently estimated parameters $\Theta^{(k)}$ and observation. x and x' in $\xi_{i,j}(x, x')$ are the state of the i -th cell and that of its one of the daughter labeled as the j -th cell, respectively. $\gamma_i(x)$ is the posterior probability of the state of the i -th cell, which is obtained by marginalization as $\gamma_i(x) = \sum_{x'} \xi_{i,j}(x, x')$. $\xi_{i,j}(x, x')$ and $\gamma_i(x)$ are computed

via Belief propagation [22]. Belief propagation makes use of the Markov property and recursively computes the posterior distributions efficiently. See Supplementary Information for the detail. In M-step, the parameters $\Theta^{(k)} = (\mathbb{T}_F, \{\theta_x^B\})$ is updated so that $\pi_B(\cdot | x)$ and \mathbb{T}_F fits the following modification of the empirical distributions(III.1):

$$\pi_{\text{emp}}^{\text{BW}}(\tau | x) := \frac{1}{\sum_{i \in \mathcal{T}_x} \gamma_i(x)} \sum_{i \in \mathcal{T}_x} \gamma_i(x) \delta(\tau - \tau_i), \quad (\text{IV.6})$$

$$\mathbb{T}_{\text{emp}}^{\text{BW}}(x' | x) := \frac{\sum_{i,j} \xi_{i,j}(x, x')}{\sum_{i,j,x'} \xi_{i,j}(x, x')}, \quad (\text{IV.7})$$

where \mathcal{T}_x is all non-leaf cells with state x in the lineage and (i, j) in the second equation runs over all the mother-daughter pairs. These are empirical distributions weighted by the posterior distributions $\gamma_i(x)$ and $\xi_{i,j}(x, x')$. For the details on the fitting process by MLE, see Supplementary Information. It is known that each update always increases the likelihood always increases [22].

V. MAIN RESULT3: APPLICATIONS

A. Numerical experiment on a toy model

We demonstrate our estimation method via a numerical experiment on a toy model. Our task is to estimate the states of the cells and parameters \mathbb{T}_F, π_F from a synthetic data (Fig. V.1 (A)). In the toy model, there are two states, fast-growth and slow-growth. We use two kinds of synthetic data. The first data do not contain any information on the states of the cell, while the second data contains information on the states of the cells at the end of lineage. We prepare the second data to compare our algorithm to that of previous research [10],

[11]. The size of a lineage fluctuates mostly between 500 to 1500. See Supplementary Information for the details.

We reconstructed the states of the cells from the synthetic data (Figure V.1 (B) and (C)). In both synthetic data, the states of the cells are reconstructed well. We checked the convergence of the log-likelihood (Figure V.2 (A), (B)). The log-likelihood converges faster in the first data than in the second data. The drop of the log-likelihood might be caused by numerical errors. We also plotted the empirical and distributions of inter-division interval (Figure V.2 (C),(D)). In both synthetic data, the empirical and the estimated distributions coincides well. We estimated \mathbb{T}_F and π_F from the second synthetic data for 1000 times to check the quality of our estimation (see Supplementary Information). We observed that our estimation is consistent with the true parameter in total. Furthermore, the estimated parameter becomes more accurate by the correction of the growth bias.

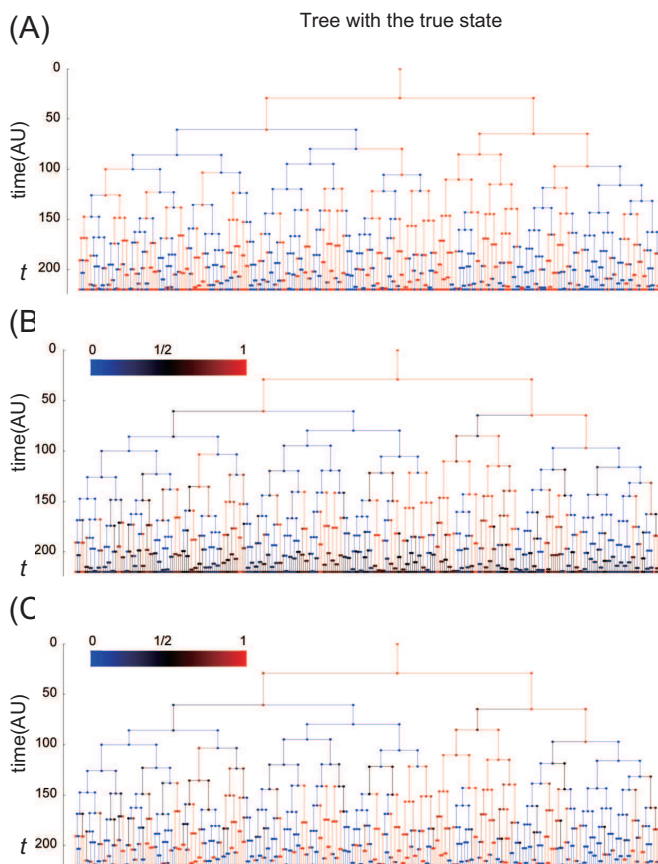


Fig. V.1: Evaluation of the algorithm by comparing a simulated lineage and the corresponding inferred states over it with and without leaves information. (A) The simulated lineage tree with the true state. (B) The lineage tree with the inferred state without the information of the states of leaves. (C) The lineage tree with the inferred state with the information of the states of leaves.

B. Determining the state of *E. coli* in a lineage

In the experiment of Hashimoto et al. [9], lineages of *E. coli* were observed via a single-cell measurement technique

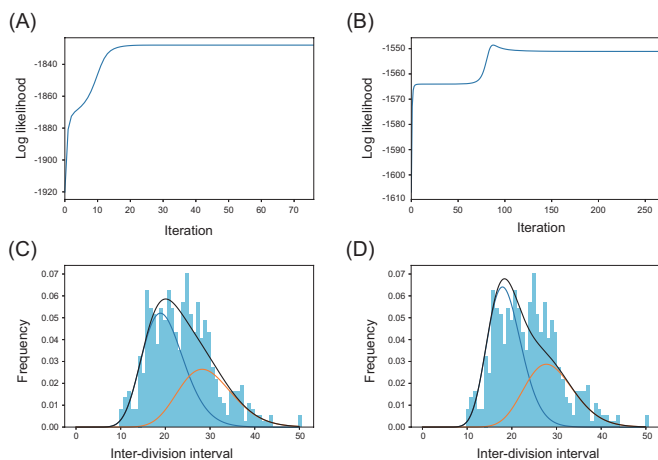


Fig. V.2: (A) The convergence of the log-likelihood when we do not know the state of the cells at the leaves (the end of lineage). (B) The convergence of the log-likelihood when we know the state of the cell at the end of lineage. (C) The empirical and the reconstructed distribution of inter-division interval when we know the state of the cell at the end of lineage. The blue and the orange line show the relative frequency of the inter-division interval of a state. The black line shows the sum of the two relative frequencies. The blue histogram shows the empirical distribution of the inter-division interval. (D) The empirical and the reconstructed distribution of inter-division interval when we do not know the state of the cell at the end of lineage.

(Figure V.3 (A)). We used the lineage data to find the states of *E. coli* which affects the growth of a population of *E. coli*. In this experiment, only a part of the lineage was observed due to the limitation of the measurement technique. We use two kinds of lineage data obtained in different experimental conditions. See [9] for the details on their experiment. Their lineage data suggest the existence of states. The inter-division interval of a parent and its daughter cell have a non-zero correlated coefficient in their experiment (See supplementary information). If there are no such states, the correlated coefficient must be zero. It contradicts to the observation and therefore there might exist states.

We first try to find such states using discrete-state model. The number of the state is determined by AIC. Especially, we first fix the number of the states and estimate the parameters. We then select the best number of the states by AIC. The estimated result is a non-state model: The number of the states selected by AIC is 1. As we mentioned before, this model cannot explain the non-zero correlated coefficients between the inter-division intervals of a parent and its daughter. The reason for this unsatisfactory result might be that discrete-state model is not appropriate to describe the population growth of *E. coli*.

We next try to determine such states using continuous-state model. The dimension k of the states $\Omega = \mathbb{R}^k$ is determined by AIC. The selected dimension is $k = 3$ (Figure V.4 (A)). The likelihood increases as the dimension does until $k = 3$.

TABLE V.1: The actual correlated coefficients of inter-division interval of a mother and the daughter cell and the estimated correlated coefficients. These two quantities coincides well.

| Experiment | Actual | estimated |
|----------------------|--------|-----------|
| F3_rpsL_Glc_37C_1min | 0.2082 | 0.2034 |
| F3_LVS4_Glc_37C_1min | 0.1095 | 0.1079 |

The posterior mean of the states of the cells in the lineage is shown in Figure V.3 (B-D). One of the 3-dimensional components (Fig. V.3 (D)) shows gradual change over the lineage, which suggests the proliferative ability of the cell is changing slowly over tens of generations. We computed the following quantities to check the quality of this reconstructed state of the cells. We first computed the posterior distribution of inter-division interval using estimated C as

$$\tau_i^{\text{pred}} = \log(Cx_i), \quad (\text{V.1})$$

where random variable x_i follows the reconstructed posterior distribution of the states of the cells. The mean of τ^{pred} behaves similarly to the observed inter-division interval (Figure V.4 (B)). Furthermore, we computed the correlated coefficients between the inter-division intervals of a parent and its daughter from the reconstructed states (see Supplementary Information). The computed correlated coefficient is almost identical to the observed correlated coefficient (Table V.1). These results validates the quality of the reconstructed states of the cells.

VI. DISCUSSION

In this study, we proposed an estimation method for lineage data. We analyzed the growth bias in a model with states and proposed a correction method. We also estimated transition matrix \mathbb{T}_F and inter-division interval distribution π_F based on BW algorithm. This method was applied to a synthetic data for validation and to lineages of *E. coli* to find the effective low-dimensional states affecting the growth of population. Our method can be applicable to a wider range of phenomena other than these examples such as microevolution, differentiation, and the acquire of the resistance to antibiotics.

As explained in section II. our model for estimation assumed (1) the independence of the state transition between the daughters and (2) all cell reproduces two cell without death. The first assumption is not essential. We can generalize the analysis of the growth bias and the explicit computation of BW algorithm to the cases where the first assumption does not hold. This generalization might be useful when we include the size of a cell as a state, which naturally correlates between the daughters. We anticipate that the analysis of the growth bias holds even if the second assumption does not hold. Our conjecture is that if a cell dies with rate $\gamma(x)$, then the empirical distributions of the generation time converges to $\pi_B(\tau | x) = \pi_F(\tau | x)e^{-(\lambda+\gamma(x))\tau}$. This π_B is again characterized as the ancestral path from a uniformly chosen cell at the end of an infinitely large lineage. Thought this conjecture is intuitive, we need further analysis to prove it.

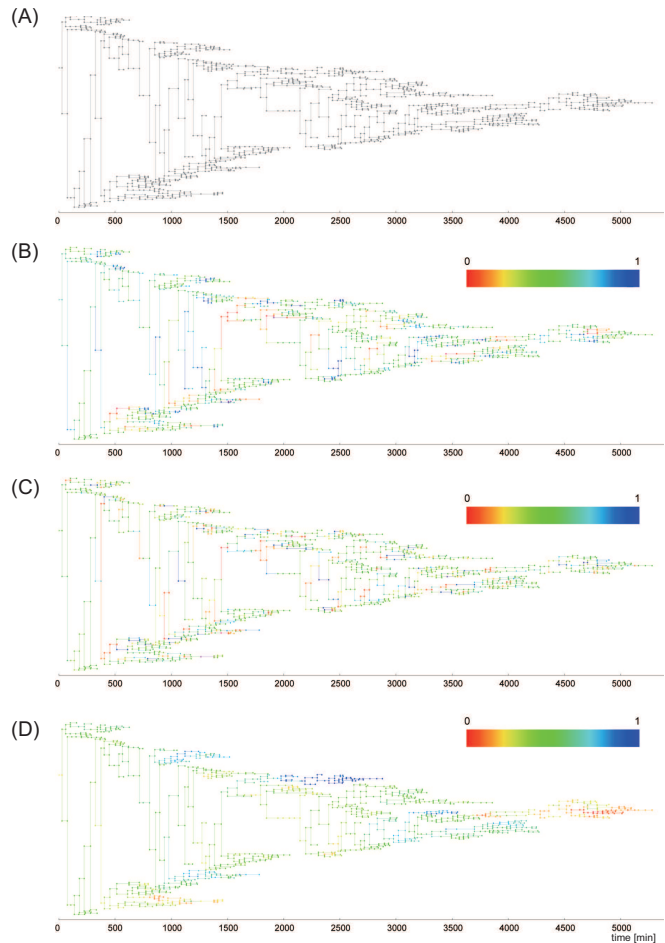


Fig. V.3: (A) The lineage of *E.coli* used for the inference. (B) The first component of the three dimension of the inferred state over the lineage. (C) The second component of the three dimension of the inferred state over the lineage. (D) The third component of the three dimension of the inferred state over the lineage.

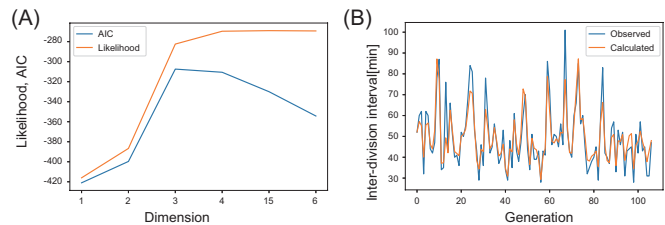


Fig. V.4: (A) The log-likelihood and AIC. The AIC is maximized when the dimension is 3. The log-likelihood seems saturate when the dimension is 3. (B) Comparison of inter-division interval. The blue line shows the actual inter-division intervals in a path of a lineage, and the orange line the predicted inter-division intervals from the reconstructed states of the cells. These two lines coincides well.

Our algorithm found the states of *E. coli* from a lineage data. These states are justified by the following facts. First, the likelihood increases as the dimension k of the model increases, and saturated at $k = 3$. This increase indicates that the estimated model captures some information on the lineage of *E. coli*. Second, the posterior distribution of the inter-division interval behaves similarly to the observed one. Finally, we computed the correlated coefficient between the inter-division intervals of a parent and its daughter from the posterior distribution of the inter-division interval. The computed correlated coefficient is almost identical to that directly computed from observation.

Our estimated model of *E. coli* have some limitations. We cannot predict the long-term behavior of the population using the estimated model. Indeed, the stationary distribution of the generation time has infinitely large variance in the estimated model. However, our model explains the short-term behavior of the population, like correlated coefficients of the inter-division interval. Our estimated model should be considered as an approximation of one-step transition of the state. In addition, the estimated states of *E. coli* are not experimentally validated. Further analysis might determine the physical realization of the states. For example, we can compute the distribution of the state at the end of lineage using estimated \mathbf{A} and posterior distributions of the states of the whole cells. We can apply invasive measurement technique of phenotypes, like Microarray, to the cells at the end of lineage. By comparing the estimated distributions of the states and the observed phenotypes, we can identify the physical realization of the state.

REFERENCES

- [1] Bigger JW (1944) Treatment of staphylococcal infections with penicillin by intermittent sterilisation. *Lancet* pp. 497–500.
- [2] Balaban NQ, Merrin J, Chait R, Kowalik L, Leibler S (2004) Bacterial persistence as a phenotypic switch. *Science* 305(5690):1622–1625.
- [3] Wakamoto Y, et al. (2013) Dynamic persistence of antibiotic-stressed mycobacteria. *Science* 339(6115):91–95.
- [4] Brock A, Chang H, Huang S (2009) Non-genetic heterogeneity – a mutation-independent driving force for the somatic evolution of tumours. *Nature Reviews Genetics* 10:336 EP –. Perspective.
- [5] Sharma SV, et al. (2010) A chromatin-mediated reversible drug-tolerant state in cancer cell subpopulations. *Cell* 141(1):69 – 80.
- [6] Ramsköld D, et al. (2012) Full-length mrna-seq from single-cell levels of rna and individual circulating tumor cells. *Nature Biotechnology* 30:777 EP –.
- [7] Shalek AK, et al. (2013) Single-cell transcriptomics reveals bimodality in expression and splicing in immune cells. *Nature* 498:236 EP –.
- [8] Rowat AC, Bird JC, Agresti JJ, Rando OJ, Weitz DA (2009) Tracking lineages of single cells in lines using a microfluidic device. *Proceedings of the National Academy of Sciences* 106(43):18149–18154.
- [9] Hashimoto M, et al. (2016) Noise-driven growth rate gain in clonal cellular populations. *Proceedings of the National Academy of Sciences* 113(12):3251–3256.
- [10] Hormoz S, Desprat N, Shraiman BI (2015) Inferring epigenetic dynamics from kin correlations. *Proceedings of the National Academy of Sciences* 112(18):E2281–E2289.
- [11] Hormoz S, et al. (2016) Inferring cell-state transition dynamics from lineage trees and endpoint single-cell measurements. *Cell Systems* 3(5):419 – 433.e8.
- [12] Olariu V, et al. (2009) Modified variational bayes em estimation of hidden markov tree model of cell lineages. *Bioinformatics* 25(21):2824–2830.
- [13] Kuzmanovska I, Miliias-Argeitis A, Mikelson J, Zechner C, Khammash M (2017) Parameter inference for stochastic single-cell dynamics from lineage tree data. *BMC Systems Biology* 11(1):52.
- [14] Chou KC, Willsky AS, Benveniste A (1994) Multiscale recursive estimation, data fusion, and regularization. *IEEE Transactions on Automatic Control* 39(3):464–478.
- [15] Laferte JM, Perez P, Heitz F (2000) Discrete markov image modeling and inference on the quadtree. *IEEE Transactions on Image Processing* 9(3):390–404.
- [16] Akaike H (1998) *Information Theory and an Extension of the Maximum Likelihood Principle*, eds. Parzen E, Tanabe K, Kitagawa G. (Springer New York, New York, NY), pp. 199–213.
- [17] Wakamoto Y, Grosberg AY, Kussell E (2011) Optimal lineage principle for age-structured populations. *Evolution* 66(1):115–134.
- [18] Marc H, Adélaïde O (2016) Nonparametric estimation of the division rate of an age dependent branching process. *Stochastic Processes and their Applications* 126(5):1433 – 1471.
- [19] Harris TE (1963) *The theory of branching processes*. (Springer-Verlag Berlin Heidelberg).
- [20] Marguet A (2016) Uniform sampling in a structured branching population. *ArXiv e-prints*.
- [21] Marguet A (2017) A law of large numbers for branching Markov processes by the ergodicity of ancestral lineages. *ArXiv e-prints*.
- [22] Christopher B (2006) *PATTERN RECOGNITION AND MACHINE LEARNING*. (Springer-Verlag New York).